Effects of additives on the non-premixed ignition of ethylene in air

Fokion N. Egolfopoulos
Aerospace & Mechanical Engineering Department
University of Southern California
Los Angeles, CA 90089–1453

and

Paul E. Dimotakis
Graduate Aeronautical Laboratories
California Institute of Technology
Pasadena, CA 91125

The ignition characteristics of heated C_2H_4 counterflowing against heated air were numerically investigated in the presence of additives such as NO, F_2, and H_2. C_2H_4 and air temperatures were chosen to resemble conditions relevant to high-Mach number, air-breathing propulsion. The numerical simulations were conducted along the stagnation streamline of the counterflow and included detailed descriptions of chemical kinetics and molecular transport. It was found that addition of NO at concentrations of about 10,000 ppm (1%), results in a substantial increase of the ignition strain rate, from 300 /s to values up to 32,000/s. This ignition promotion is caused by enhanced radical production that is initiated through the interaction between NO and HO_2. A further increase in the NO amount leads to reduced improvements. Small additions of F_2 and H_2 were also found to promote ignition, but to lesser extent compared to NO. Results also show that with the addition of F_2 in the presence of NO, ignition promotion is further enhanced, and for F_2 and NO concentrations larger than 25,000 ppm, the system becomes hypergolic. The present investigations suggest that the use of C_2H_4, NO, and F_2 may permit ignition at conditions of relevance to SCRAMJET's.

1. Introduction

The use of hydrocarbons for high Mach number, air-breathing propulsion was recently addressed (*e.g.*, Edwards 1996). The concept pertains to flight Mach numbers and (static) temperatures in the range,

$$4 \lesssim M_\infty < 8 , \qquad 250\,\mathrm{K} < T_\infty < 300\,\mathrm{K} , \tag{1}$$

where, for a perfect gas, we may expect temperatures of,

$$T_0 = \left[1 + r \left(\frac{\gamma - 1}{2} \right) M_\infty^2 \right] T_\infty . \tag{2a}$$

In this expression, $\gamma \equiv c_p/c_v$ the ratio of specific heats (here assumed constant) and r a temperature-recovery factor. The latter ranges from unity for stagnation flow, to $\sim Pr^{1/3}$ for turbulent boundary-layer wall recovery ($Pr \simeq 0.7$, for air, is the Prandtl number), to $\sim Pr^{1/2}$ for laminar boundary-layer wall recovery. Such temperatures may be expected for (near-)adiabatic conditions, but could be lowered by heat transfer and active cooling. For expected M_∞ and T_∞ conditions (Eq. 1), we then expect,

$$1000\,\mathrm{K} \lesssim T_0 \lesssim 4000\,\mathrm{K} , \tag{2b}$$

necessitating the use of endothermic fuels to cool the fuselage and internal-flow passages for flights of any duration (Egolfopoulos & Dimotakis 1998, hereafter referred to as 'ED98').

The lower limit of the envisaged M_∞ range is set by the ignition and flame stability characteristics of hydrocarbons, while the upper limit is set by the cooling ability of such fuels. Whether the proposed concept is realizable, depends critically on the ability to achieve and sustain ignition in a flow environment characterized by very high strain rates, imposed by large velocity gradients across air-fuel mixing layers. In this environment, strain rates of the order of $10^4 - 10^6$/s are expected (*e.g.*, Egolfopoulos *et al.* 1996). Non-premixed hydrocarbons do not ignite nor sustain vigorous burning under such conditions (*e.g.*, Fotache *et al.* 1997a, 1997b; Egolfopoulos *et al.* 1997).

In the proposed hydrocarbon-fueled SCRAMJET concept, heat added to typical jet fuels in the course of endothermic cooling will result in fuel temperatures that will cause thermal cracking. At the expected sustained elevated fuel temperatures, the extent of cracking may be such that near-equilibrium compositions are attained. Thus, products of full, or partial, cracking will be fed into the combustor. As a result, ignition behavior will be that of a fuel blend of lower molecular weight constituents. While the elevated temperatures of such fuel blends will promote ignition, it is not clear whether that alone is sufficient and what the combined effect of the various components will be.

The ED98 numerical study focused on the non-premixed ignition of fuel blends that may result from the thermal cracking of $C_{12}H_{26}$, a representative constituent of kerosene-type fuels. For fuel temperatures in the range, $800\,\mathrm{K} < T_{\mathrm{fuel}} < 1050\,\mathrm{K}$ (*cf.* Eq. 2), equilibrium calculations revealed that the fuel blend composition is largely controlled by nearly-equal amounts of CH_4 and C_2H_4, with smaller amounts of H_2, C_2H_2, C_2H_6, and $C_3 - C_4$ hydrocarbons also present. The results confirmed that the ignition process is particularly sensitive to air temperature, T_{air}, and is greatly facilitated at the higher T_{air}'s that correspond to the higher M_∞'s (*cf.* Eqs. 1 and 2). $T_{\mathrm{fuel}} = 950\,\mathrm{K}$ and $p = 1\,\mathrm{atm}$ was assumed throughout the study. The study also revealed that ignition behavior is controlled by the synergistic effect of CH_4 and C_2H_4, with CH_4 inhibiting ignition of C_2H_4 at the higher T_{air} values. For (the lower value) of $T_{\mathrm{air}} = 1050\,\mathrm{K}$, however, small additions of CH_4 were found to moderately promote the ignition process. Large additions of CH_4 inhibited C_2H_4 ignition under all conditions investigated. For the less favorable $T_{\mathrm{air}} = 1050\,\mathrm{K}$, that corresponds to the lower limit of the proposed M_∞ range, ignition strain rates, σ_{ign}, of such fuel blends were found to be of the order of $10^2/\mathrm{s}$ to $10^3/\mathrm{s}$, substantially lower than anticipated strain rates in a SCRAMJET.

In order to increase the values of σ_{ign} for the lower $T_{\mathrm{air}} = 1050\,\mathrm{K}$ case, additives such as H_2 and F_2 were independently supplemented into the fuel and air streams, respectively. As expected, addition of H_2 promoted ignition and values of $\sigma_{\mathrm{ign}} \simeq 4,000/\mathrm{s}$ were found for a 10% molar fraction of H_2 in the fuel-blend. Similarly, a 1% molar fraction of F_2 in the air stream resulted in a similar value of $\sigma_{\mathrm{ign}} \simeq 4,000/\mathrm{s}$. While ignition promotion through H_2 addition was found to be caused by efficient

H-radical production, ignition promotion through F_2 addition was found to result from the additional fuel consumption by F-radicals.

Hydrocarbon oxidation is also known to be promoted in the presence of NO and extensive pertinent studies in homogeneous systems and flames have been conducted (*e.g.*, Bromly *et al.* 1992, Doughty *et al.* 1996, Law 1998, Marinov *et al.* 1998, Nelson *et al.* 1994, Tan *et al.* 1999). The main mechanism supporting the observed oxidation promotion, is NO reactions with RO_2, where R = H, or an alkyl group, that produce RO and NO_2 (*e.g.*, Doughty *et al.* 1996). Subsequently, RO can decompose to H radicals that are essential to the overall oxidation process. For the special case of NO reacting with HO_2, OH radicals, which are very effective in consuming hydrocarbons, are readily produced. Thus, through these NO-induced reactions, highly-reactive OH and H radicals are readily produced from the relatively unreactive RO_2 radicals. These studies have also revealed that the extent of the observed oxidation promotion depends on the hydrocarbon type. For example, the recent flow reactor study of Marinov *et al.* (1998) has shown that C_2H_4 and C_3H_8 interact more effectively with NO, compared to CH_4. The also recent flame-ignition studies of Law and coworkers (Law 1998, Tan *et al.* 1999) revealed that the presence of NO reduces the ignition temperature of hydrocarbons, with CH_4 and C_3H_8 being more sensitive to NO addition, compared to C_2H_6 and $i-C_4H_{10}$.

The ignition studies of Law and coworkers (Law 1998, Tan *et al.* 1999) assessed the behavior of selected saturated hydrocarbons and H_2. The ignition/extinction characteristics of C_2H_4 and its blends with other cracked-fuel hydrocarbons, as well as the effects of such additives as H_2 and F_2, and NO were studied by ED98. The ignition sensitivity of pure C_2H_4 to additives was not examined in these studies. C_2H_4 is a main constituent of thermal cracking of jet fuel, with ignition characteristics that are superior to those of CH_4, the other main constituent. Thus, if ignition strain rates approriate for SCRAMJET operation are to be achieved, C_2H_4 must be independently considered.

The main objective of this work is to extend previous studies by considering the non-premixed ignition/extinction characteristics of additives, such as NO, on pure C_2H_4, for temperatures of relevance to SCRAMJET's. NO is expected to have a noticeable effect in promoting C_2H_4 ignition, as was reported by Marinov

et al. (1998). Furthermore, NO can be inherently present in, or added to, air with effects on engine materials that are benign compared to F_2. The study also assesses the relative effect of NO and other additives on pure C_2H_4 ignition, such as F_2 and H_2.

2. Numerical method

The main effects of the imposed flow environment on ignition can be quantified in opposed-jet configurations in terms of the hydrodynaamic strain rate, defined as the maximum absolute value of the velocity gradient on the air side, just before the ignition kernel, *i.e.*,

$$\sigma \equiv \left| \frac{\partial u}{\partial x} \right|_{\text{max, air side}} . \tag{3}$$

The air side is chosen for the definition of σ, as the rate of transport of O_2 in the hydrodynamic zone determines the extent of its leakage through the main reaction zone. This quantity is well-defined and can be well-controlled (*cf.* Kreutz & Law 1996 and Fotache *et al.* 1997a, 1997b).

An additional advantage of this configuration is that the flow-field is quasi one-dimensional in the vicinity of the centerline. Thus, the simulations are conducted by solving the one-dimensional, steady, conservation equations of mass, momentum, energy, and species concentrations along the stagnation streamline. The pertinent equations and boundary conditions can be found in Egolfopoulos (1994a) and Egolfopoulos & Campbell (1996).

Similarly to the ED98 study on non-premixed hydrocarbon ignition, the original stagnation-flow code (Kee 1990), subsequently modifed for non-premixed flames (Egolfopoulos 1994b), was further modified by implementing a two-point continuation approach to capture the entire S-curve behavior (*e.g.*, Williams 1985). This approach was first introduced by Nishioka *et al.* (1996) and imposes a pre-determined temperature, or species mass fraction reduction, at two points in the flow field. Thus, the strain rate is solved for, rather than imposed as a boundary condition. Locations where the temperature or species concentrations have maximum slopes were chosen to be the two points, following the recommendations of Nishioka *et*

al. (1996). In the present study, the two-point continuation approach is applied to H radicals, although any other radical can be used (Nishioka *et al.* 1996). A steady solution is first established under conditions of vigorous burning at relatively low strain rates. Subsequently, H-radical mass fraction is incrementally reduced, permitting all S-curve branches, stable and unstable, to be determined.

	Reaction	A	n	E_a	Ref.
R295	$NO + F_2 \rightarrow FNO + F$	4.20E11	0.00	2285	1
R296	$NO + F + M \rightarrow FNO + M$	3.00E16	0.00	0	1
R297	$H + F_2 \rightarrow HF + F$	2.90E09	1.40	1325	1
R298	$F + H_2 \rightarrow HF + H$	2.70E12	0.50	634	1
R299	$F_2 + M \rightarrow F + F + M$	2.10E13	0.00	33700	1
R300	$HF + M \rightarrow H + F + M$	1.10E19	-1.00	134100	1
R301	$C_2H_4 + F \rightarrow C_2H_3 + HF$	1.00E14	0.00	2000	2
R302	$C_2H_3 + F \rightarrow C_2H_2 + HF$	2.00E13	0.00	0	3
R303	$C_2H_2 + F \rightarrow C_2H + HF$	5.00E13	0.00	0	4
R304	$OH + F \rightarrow O + HF$	2.00E13	0.00	0	3
R305	$HO_2 + F \rightarrow O_2 + HF$	2.89E12	0.50	0	3
R306	$H_2O + F \rightarrow OH + HF$	1.30E09	1.50	0	3
R307	$H_2O_2 + F \rightarrow HO_2 + HF$	1.73E12	0.50	0	3
R308	$CH_3 + F \rightarrow CH_2(s) + HF$	1.62E16	-0.88	-981	3
R309	$CH_4 + F \rightarrow CH_3 + HF$	5.90E12	0.50	450	3
R310	$CH_3OH + F \rightarrow CH_3O + HF$	2.62E09	1.44	-205	3
R311	$CH_3OH + F \rightarrow CH_2OH + HF$	4.62E07	1.97	-300	3
R312	$CH_2O + F \rightarrow HCO + HF$	6.00E13	0.00	2000	3
R313	$CH_3O + F \rightarrow CH2O + HF$	3.00E13	0.00	0	3
R314	$HCO + F \rightarrow CO + HF$	1.00E13	0.00	0	3
R315	$C_2H_6 + F \rightarrow C_2H_5 + HF$	8.00E12	0.00	300	3

Table 1. $H_2/NO/F_2$/hydrocarbon/O_2 parameters: $k = A\,T^n\,e^{-E_a/RT}$, A in mol-cm-s, E_a in cal/mol. Refs 1: Egolfopoulos *et al.* (1996), 2: Wang & Frenklach (1997), 3: Burgess *et al.* (1997), and 4: Westmoreland (1997).

The code was integrated into the CHEMKIN (Kee *et al.* 1989) and Transport (Kee *et al.* 1983) subroutine packages. The kinetic mechanism of Wang & Frenklach (1997), with 50 species and 294 reactions, was adopted. This mechanism describes the oxidation characteristics of C_1- and C_2-hydrocarbons and N_2-related chemistry,

and was developed for C_2H_4 and C_2H_2 flames, while retaining the main features of the GRI 2.1 mechanism (Bowman *et al.* 1995). The use of the Wang & Frenklach mechanism is essential, as the GRI 2.1 mechanism does not include the CH_2CHO (vinyoxy) radical species that plays an essential role in C_2H_4 ignition. It was found in ED98 that omitting CH_2CHO and its reactions leads to an underestimation of the ignition strain rate, $\sigma_{\rm ign}$, by a factor of 30, or so. The Wang & Frenklach mechanism is augmented by four species (F_2, FNO, HF, and F) and 21 reactions (Table 1) that describe couplings between H_2, hydrocarbons, NO, and F_2. This was motivated by the results of previous experiments (Mungal & Dimotakis 1984) and numerical-simulation studies (Egolfopoulos *et al.* 1996), where the simultaneous presence of small quantities of F_2 and NO was found to enhance overall radical production. Reactions between hydrocarbons and F_2 are taken from Burgess *et al.* (1997) and Westmoreland (1997). Reactions between the F_2 and NO are adopted as in Egolfopoulos *et al.* (1996).

3. Results and discussion

Similarly to the ED98 ignition study, the simulations are conducted for $T_{\rm fuel} = 950\,{\rm K}$. Air temperature is chosen to be $T_{\rm air} = 1050\,{\rm K}$, for which ignition characteristics thermal cracking products, including C_2H_4, are rather poor. Details of the ignition process and the controlling mechanisms are identified by conducting structure, sensitivity, reaction-path, and integrated species-consumption path analyses in the vicinity of the "ignition kernel", as originally identified by Kreutz & Law (1996). The details of the sensitivity analysis in flames are described by Kee *et al.* (1985). The integrated species-consumption path analysis is obtained by a spatial integration of the species-consumption rates and by subsequent identification of the dominant kinetic paths. The response of the reacting non-premixed system to σ (Eq. 3) is presented through the variation of the maximum H-radical mass fraction, $(Y_{\rm H})_{\rm max}$, with σ.

3.1 S-curve response of C_2H_4/air

The S-curve response of C_2H_4/air is shown in Fig. 1. Point A denotes a condition of vigorous burning, B extinction, E ignition, and F a pre-ignition condition characterized by low overall reaction intensity. Points C and D are located in the unstable branch of the S-curve and resemble conditions of "intermediate" stages of (unstable) ignition and extinction respectively. The detailed response of the $\sigma_{\rm ign}$ to $T_{\rm air}$ (results from ED98) is shown in the inset in Fig. 1, with symbols denoting values determined from the simulations and the solid line a smooth least-square-fit to aid the eye. The large sensitivity of $\sigma_{\rm ign}$ to $T_{\rm air}$ is evident.

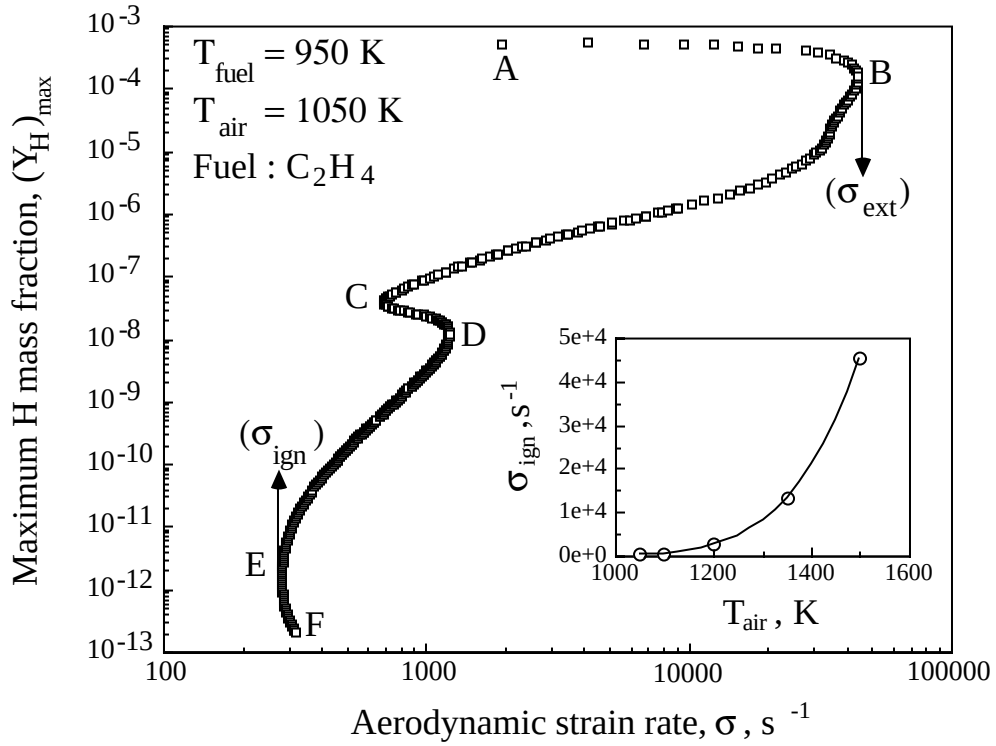

FIG. 1 S-curve response of C_2H_4/air ($T_{\rm air} = 1050\,{\rm K}$, $T_{\rm fuel} = 950\,{\rm K}$). Inset figure plots $\sigma_{\rm ign}$ (circles) with least-square smooth fit curve to aid the eye (ED98).

The dominant mechanisms of the various S-curve branches are revealed by the structure of the ignition kernel. As reported in the ED98 study, in the pre-ignition Region F, C_2H_4 is largely consumed through reactions (numbers correspond to the order in which the reactions appear in the kinetic mechanism),

R165 (30%) $\qquad C_2H_4 + O \longrightarrow CH_3 + HCO$,

R167 (18%) $C_2H_4 + CH_3 \longrightarrow C_2H_3 + CH_4$,

R166 (16%) $C_2H_4 + OH \longrightarrow C_2H_3 + H_2O$,

R163 (16%) $C_2H_4 + H + M \longrightarrow C_2H_5 + M$.

CH_3 produced by R165 is largely consumed by R167. Thus, C_2H_3 is the main product of C_2H_4 consumption. C_2H_3 is consumed by the low-activation-energy reactions,

R160 (53%) $C_2H_3 + O_2 \longrightarrow CH_2CHO + O$,

R161 (44%) $C_2H_3 + O_2 \longrightarrow HCO + CH_2O$.

vinyoxy radical, CH_2CHO, is entirely decomposed through the reaction ('-' denotes reverse reaction),

R182- (100%) $CH_2CHO + M \longrightarrow CH_2CO + H + M$,

that is the main source of H radicals. H radicals, in turn, are consumed by R163(60%) and the main branching reaction,

R1 (20%) $H + O_2 \longrightarrow OH + O$,

that produces the O and OH radicals essential for fuel consumption and, thus, ignition.

Given the importance of H-radicals to the ignition process, as they are essential for the progress of R1, we may conclude that the kinetics of CH_2CHO play a crucial role in the pre-ignition Region F. The omission of such species result in substantial underprediction of $\sigma_{\rm ign}$ of C_2H_4 (*cf.* ED98).

The chemical-kinetic processes in the pre-ignition Region F are quite slow compared to the transport processes the extent of which is imposed by the fluid mechanics. As σ is reduced, Point E is eventually reached, where the rate of radical production exceeds the convective/diffusive radical loss rate out of the ignition kernel (Kreutz & Law 1996), and ignition occurs. At Point E, C_2H_4 is entirely consumed by H, O, OH, and CH_3 radicals, with virtually no heat release. Thus, for the present reactant initial conditions, C_2H_4 ignition is caused by radical runaway rather than thermal runaway, similarly to H_2 (Kreutz & Law 1996). This

is physically reasonable, as the reactions responsible for C_2H_4 consumption and H-radical production are characterized by low activation energies. The sensible energy supplied by the reactant streams is sufficient for the effective progress of the radical-producing reactions and no additional heat release is required.

The non-monotonic behavior of the S-curve at Points C and D was also assessed. While these conditions are physically unstable, they are possible (mathematical) solutions. It was found that between Regions F and D the contribution of R166 to fuel consumption, *i.e.*, through OH, increases by following the solution path from Region F and moving towards D, with R166 the main fuel-consuming reaction as the radical pool increases. Within this region, the contribution of R1 to OH production is reduced at the higher radical concentrations, as substantial amounts of H_2O_2 are produced through the radical-radical recombination reaction,

R23 $$HO_2 + HO_2 + M \longrightarrow H_2O_2 + M \ ,$$

radical-radical reactions are unimportant for low radical concentrations. Subsequently, H_2O_2 readily decomposes to $2\,OH$ through the reaction,

R16 $$H_2O_2 + M \longrightarrow 2\,OH + M \ .$$

Thus, the contribution of R16 to OH production monotonically increases, over that of R1 at higher radical concentrations, with the kinetics of HO_2 and H_2O_2 controlling the system response. Given the low diffusivity of these species, steady solutions are obtained at lower values of σ and that explains the turning behavior in Region D. At this point, the maximum rate of R23 is equal to that of R1. As Point C is approached, intensified OH production results in heat release that further facilitates the decomposition reaction R16. Just before Point C, the maximum rate of R16 exceeds that of R1 and as Point C is reached, OH production is such that sufficient heat is released to cause this ignition-type, turning-point behavior. The variation of the maximum reaction rates of R1, R16, and R23 is shown in Fig. 2.

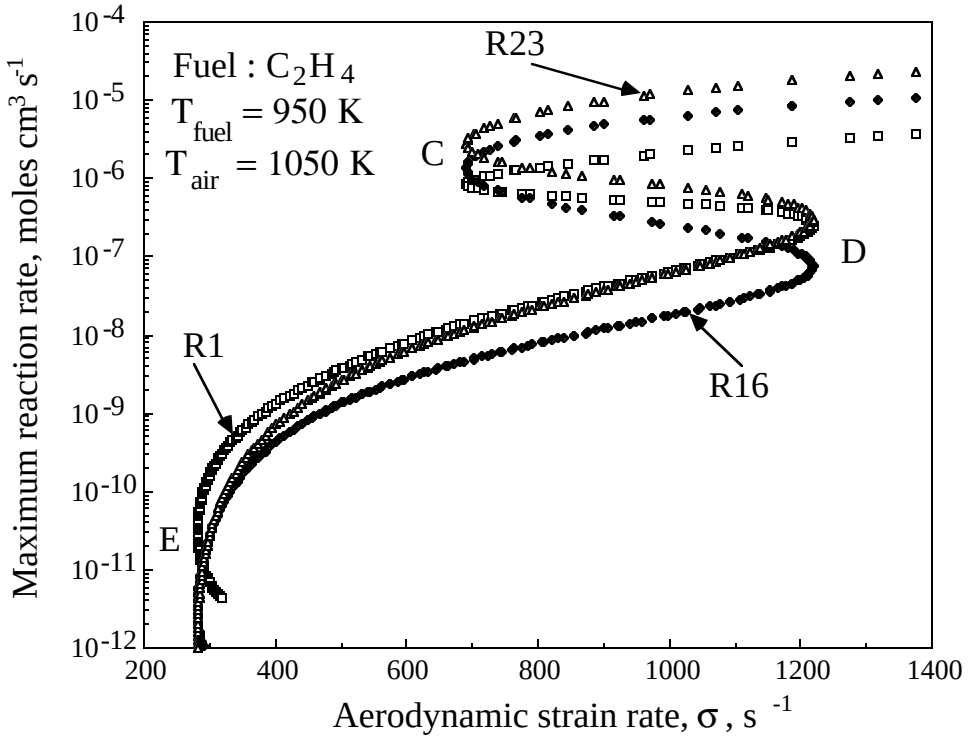

FIG. 2 Effect of strain rate on the maximum rates of Reactions R1, R16, and R23 for C_2H_4/air ($T_{\text{air}} = 1050\,\text{K}$, $T_{\text{fuel}} = 950\,\text{K}$.

3.2 NO addition

The effect of NO as an additive was investigated by adding it in amounts ranging from 500 to 50,000 ppm, on a molar basis, into the reactant streams. The resulting S-curves are shown in Figs. 3 and 4, for NO additions into the air and fuel streams, respectively.

As can be seen, the presence of NO causes a substantial increase of σ_{ign}, especially when NO is added on the air side. For example, addition of 500 ppm of NO increases the σ_{ign} by a factor of 8, while σ_{ign}'s as high as 32,000/s are achieved with NO additions up to 10,000 ppm. Through NO addition, ignition takes place at higher radical concentrations corresponding to the Region C-D of Fig. 1. As mentioned above, in the absence of NO, this region represents an unstable-ignition regime. Furthermore, these higher radical concentrations result in noticeable heat release that becomes a factor in the ignition process. It is also seen that NO can affect extinction as well, especially when added on the air side.

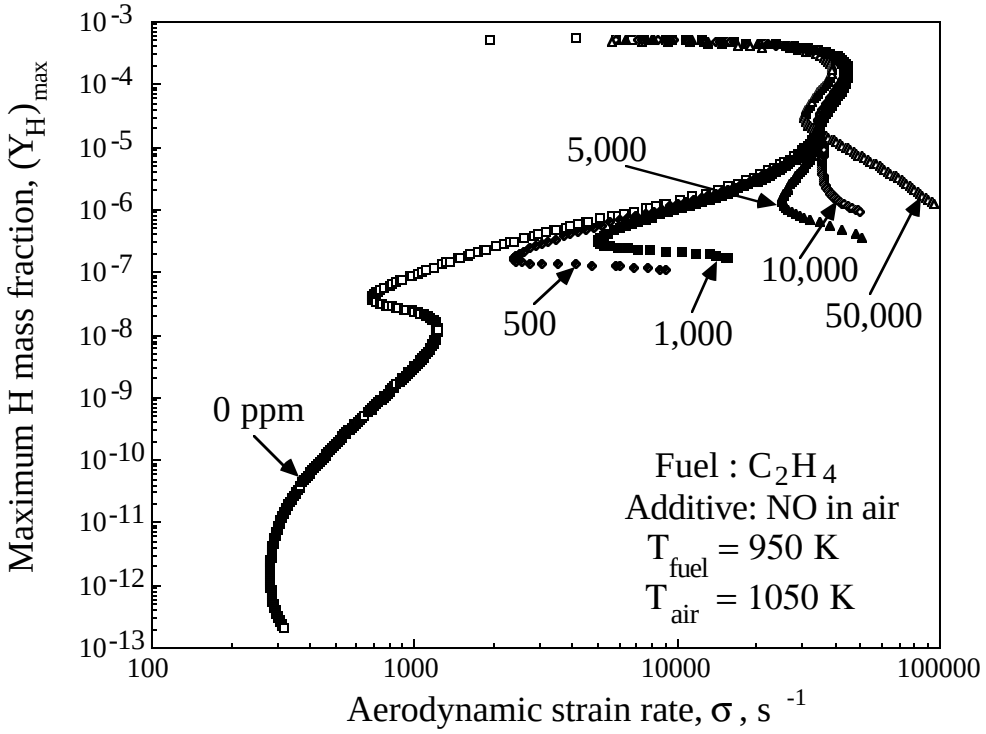

FIG. 3 Effect of NO addition on S-curve response of C_2H_4/air ($T_{\rm air} = 1050\,$K, $T_{\rm fuel} = 950\,$K). NO added to air stream.

Figures 5a and 5b depict the variation of $\sigma_{\rm ign}$ and the extinction strain rate, $\sigma_{\rm ext}$, respectively, with NO addition. Figure 5a shows that the sensitivity of $\sigma_{\rm ign}$ to NO is high up to about 10,000 ppm. For larger amounts of NO, the values of $\sigma_{\rm ign}$ level off when NO is added on the fuel side, while a moderate reduction in $\sigma_{\rm ign}$ is observed when NO is added on the air side. Furthermore, for additions below 10,000 ppm, NO is more effective in increasing $\sigma_{\rm ign}$ when added on the air side. Figure 5b also shows that when NO is added on the air side, $\sigma_{\rm ext}$ moderately increases for small amounts (*i.e.*, $<$ 1000 ppm), while noticeably decreasing for larger amounts of NO. NO addition on the fuel side results in a moderate increase of $\sigma_{\rm ext}$, which remains nearly-constant for amounts up to 50,000 ppm.

The effect of NO on ignition was analyzed for 5,000 ppm and 50,000 ppm added on the air side. The 5,000 ppm case was chosen as representative of the promoting behavior of NO on ignition. The 50,000 ppm case was chosen to study the reduced promoting effect of NO, when added in large amounts.

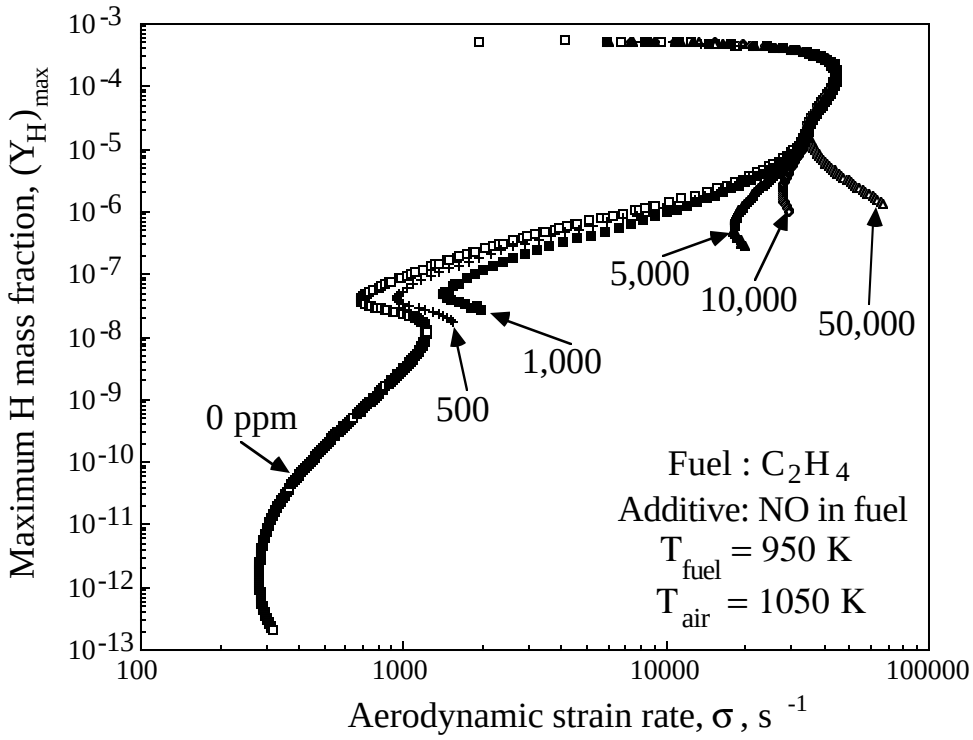

FIG. 4 Effect of NO addition on S-curve response of C_2H_4/air ($T_{\rm air} = 1050\,$K, $T_{\rm fuel} = 950\,$K). NO added to fuel stream.

At ignition for the 5,000 ppm case, C_2H_4 is consumed through R166(47%), R165(28%), and R163 (19%). It is apparent that OH is largely responsible for the fuel consumption, with a role that is substantially enhanced, as compared to the case of pure C_2H_4 ignition, described earlier. This behavior is attributable to a sequence of reactions with NO that results in the enhancement of OH-radical production. More specifically, OH is produced through reactions,

R91 (35%) $\quad CH_3 + HO_2 \longrightarrow CH_3O + OH\,,$

R201 (28%) $\quad NO + HO_2 \longrightarrow NO_2 + OH\,,$

R204 (16%) $\quad NO_2 + H \longrightarrow NO + OH\,,$

R19 (13%) $\quad H + HO_2 \longrightarrow OH + OH\,.$

At the same time, NO is entirely (97%) consumed through R201.

Thus, NO is converted to NO_2 through R201 and is, subsequently, reduced back to NO through R204. This cyclic, "catalytic" behavior of NO has been noted

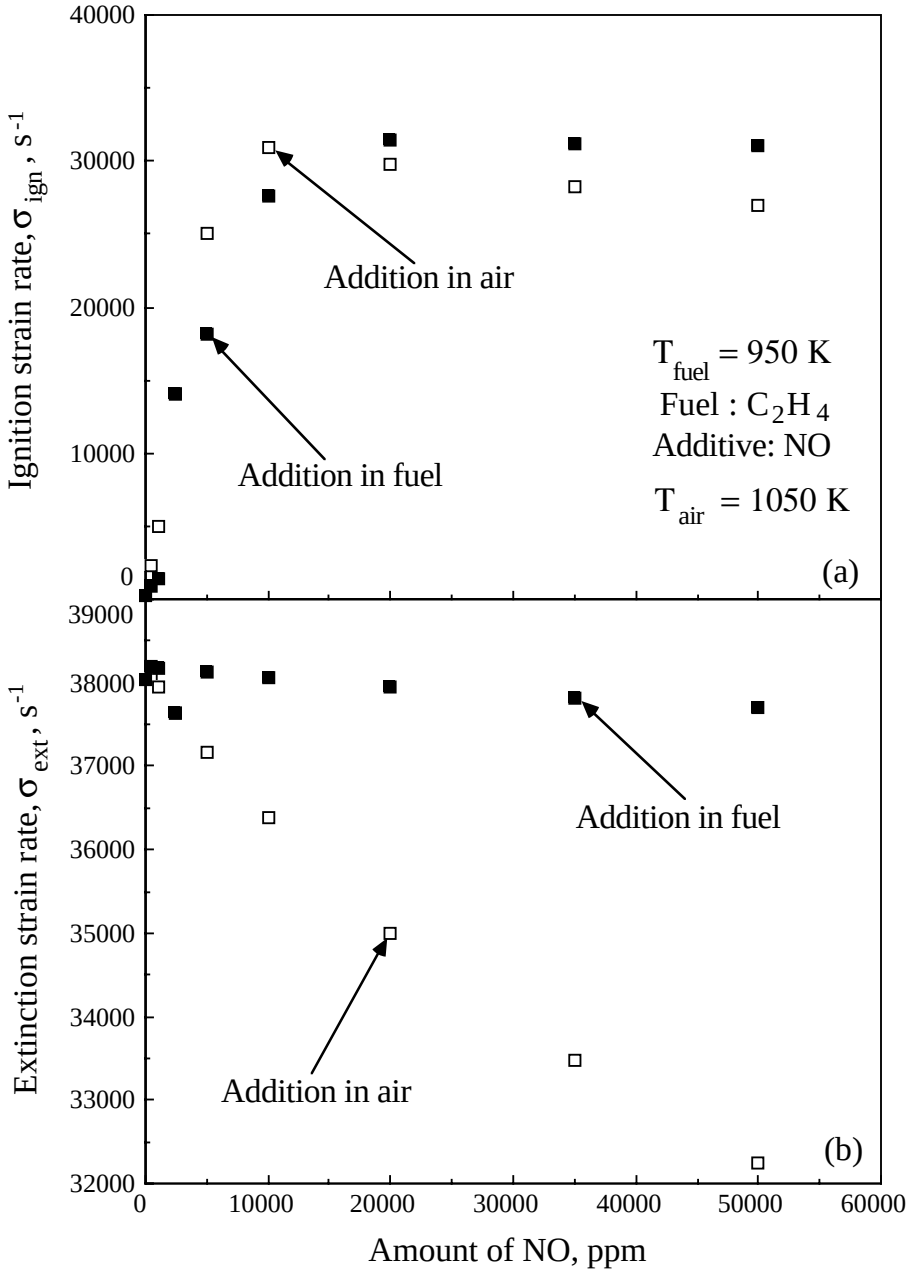

FIG. 5 Effect of NO addition on (a) $\sigma_{\rm ign}$ and (b) $\sigma_{\rm ext}$ of C_2H_4/air ($T_{\rm air} = 1050\,{\rm K}$, $T_{\rm fuel} = 950\,{\rm K}$).

previously (*e.g.*, Bromly *et al.* 1992, Doughty *et al.* 1996, Law 1998, Marinov *et al.* 1998, Nelson & Haynes 1994, Tan *et al.* 1999), and enhances production of the fuel-scavenger OH radicals. It is noteworthy that R201 and R204 are responsible for an overall, NO-induced, branching-like reaction, $H + HO_2 \rightarrow 2OH$, which can also proceed as an elementary step through R19, independently of NO. This point

was further assessed by determining that HO_2 is consumed through R91(34%), R201(28%), and R19(13%). As a result, the NO is responsible for a more effective conversion of HO_2 to OH radicals, as compared to R19.

Marinov *et al.* (1998) indicated that C_2H_4 ignition is particularly sensitive to NO addition because of the efficient production of HO_2 radicals during the C_2H_4 oxidation. More specifically, at the ignition point, HO_2 is largely produced by the reaction (the percentage here refers to HO_2-production contribution),

R50 (75%) $\qquad HCO + O_2 \longrightarrow CO + HO_2$,

so that the HO_2 production rate directly depends on HCO concentration. As C_2H_4 is consumed, C_2H_3 is produced and oxidized through R161 to HCO and CH_2O. Subsequently, CH_2O reacts with OH through the reaction,

R79 $\qquad CH_2O + OH \longrightarrow HCO + H_2O$.

Thus, per C_2H_4 molecule consumed, two molecules of HO_2 may form (Marinov *et al.* 1998).

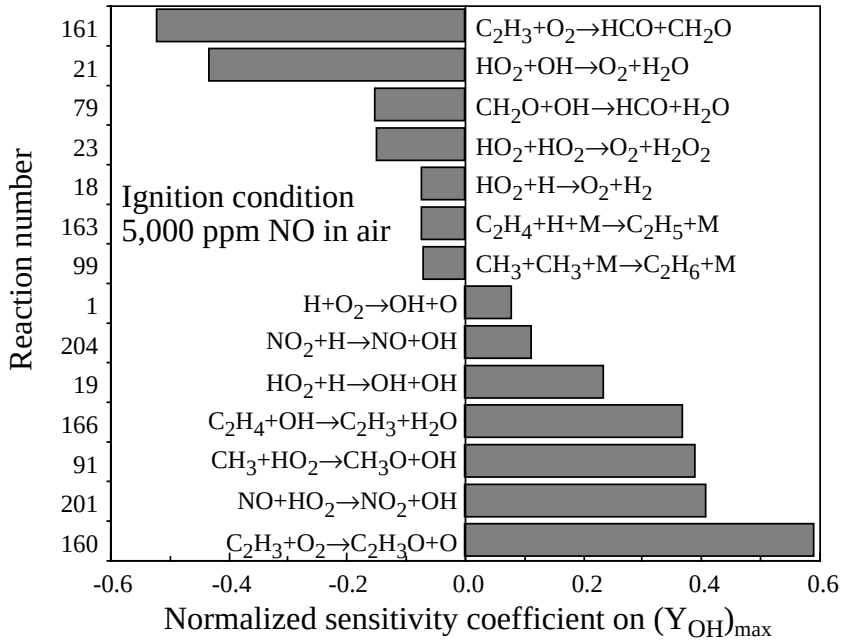

FIG. 6 Normalized sensitivity coefficients on $(Y_{OH})_{max}$ at the ignition condition of C_2H_4/air, with 5,000 ppm NO addition to the air stream (T_{air} = 1050 K, T_{fuel} = 950 K).

Figure 6 depicts the normalized sensitivity coefficients of the most important reactions on the maximum mass fraction of OH radicals, $(Y_{OH})_{max}$, at the ignition condition with 5,000 ppm NO addition to the air stream. The vertical axis denotes the reaction number as it appears in the mechanism. The effect of R160, R201, R91, R166, R19, and R204 on OH-production promotion can be seen to be large. As also shown earlier, the sensitivity to R201 is greater compared to R19. We also note that while R166 appears to be an OH sink, its net effect on overall OH production is large. It largely consumes C_2H_4, a process essential for the overall radical pool increase. Reactions R23, R161 and,

R21 $$HO_2 + OH \longrightarrow O_2 + H_2O \ ,$$

R79 $$CH_2O + OH \longrightarrow HCO + H_2O \ ,$$

have a significant retarding effect on OH production. In R21 and R79, HO_2 radicals are consumed and this is in competition with R201. OH radicals are also consumed in R21 and R79, and this is in competition with R166.

At the ignition point for the 50,000 ppm case, C_2H_4 is consumed through reactions R166(29%), R165(24%), and

R164 (40%) $$C_2H_4 + H \longrightarrow C_2H_3 + H_2 \ .$$

The role of OH in fuel consumption is reduced at this larger NO addition. However, it is still enhanced as compared to the pure C_2H_4 case. For large additions, NO is only partially consumed by R201(44%), as additional consumption is caused through reaction,

R289 (38%) $$NO + HCCO \longrightarrow HCNO + CO \ ,$$

so that the effective OH-production sequence is not fully utilized. This inhibiting effect of R289, for large NO additions, was also reported by Nelson & Haynes (1994). The reduced contribution of R201 in consuming NO is a result of the reduction of HO_2 concentration. HO_2 is readily produced through O_2 reactions with the HCO and C_2H_5 radicals. Addition of large amounts of NO causes the O_2 concentration in the oxidizer to be reduced. Thus, the rate of HO_2 production is reduced. HCCO is largely produced from CH_2CO reactions with H and OH, while CH_2CO is produced

by R182-. HCNO entirely isomerizes to HNCO by reacting with H, and HNCO is consumed through reaction,

R280 (80%) $\qquad$ $\mathrm{HCNO + H \longrightarrow NH_2 + CO}$.

Through this alternative NO-consumption sequence, NH_2 and CO are produced, that have no particular promoting effect on ignition. Thus, as NO is added in progressively larger amounts, the role of R289 is enhanced, over that of R201, and its promoting effect on ignition is reduced.

The effect of NO addition on σ_{ext} was also assessed when NO is added to the air stream. The analysis showed that there are two competing mechanisms, namely OH-radical production through R201 and O_2 concentration reduction as more NO is added. Extinction, being a high-temperature phenomenon, is particularly sensitive to the progress of the high activation energy, branching-reaction R1, whose rate is directly proportional to O_2 concentration. The radical-producing mechanism initiated by R201 results in a moderate increase of σ_{ext} for NO additions below 500 ppm. For larger amounts, the dilution effect of NO dominates, resulting, thus, in a noticeable reduction of σ_{ext}. The effect of O_2-dilution is not as strong on ignition, which does not depend to the same extent on R1, as ignition is a lower-temperature, radical-deficient phenomenon.

The structure of the ignition and extinction points were also analyzed when NO is added on the fuel side. Cases of small and large NO additions were considered. For small amounts, with NO added to the fuel side, its effectiveness in producing OH radicals is reduced relatively to the addition on the air side. R201 is a key one in OH radical production and its rate is proportional to the molar concentrations of NO and HO_2. Given that HO_2 is largely produced in the oxygen-rich part of the domain, when NO is supplied to the fuel stream, the net rate of R201 is lower compared to when NO is added to the air stream. Figure 7 depicts results obtained from structure analysis for the ignition points corresponding to 5,000 ppm NO addition to the fuel and air streams. The spatial coordinate has been replaced by appropriate progress variables. Figure 7a shows the variation of the mass fraction of HO_2, $Y_{\mathrm{HO_2}}$, with Y_{NO}, the NO mass fraction. We find that when NO is added on the fuel side, the $Y_{\mathrm{HO_2}}$ maximum occurs in a regime of lower Y_{NO} values as compared to the case

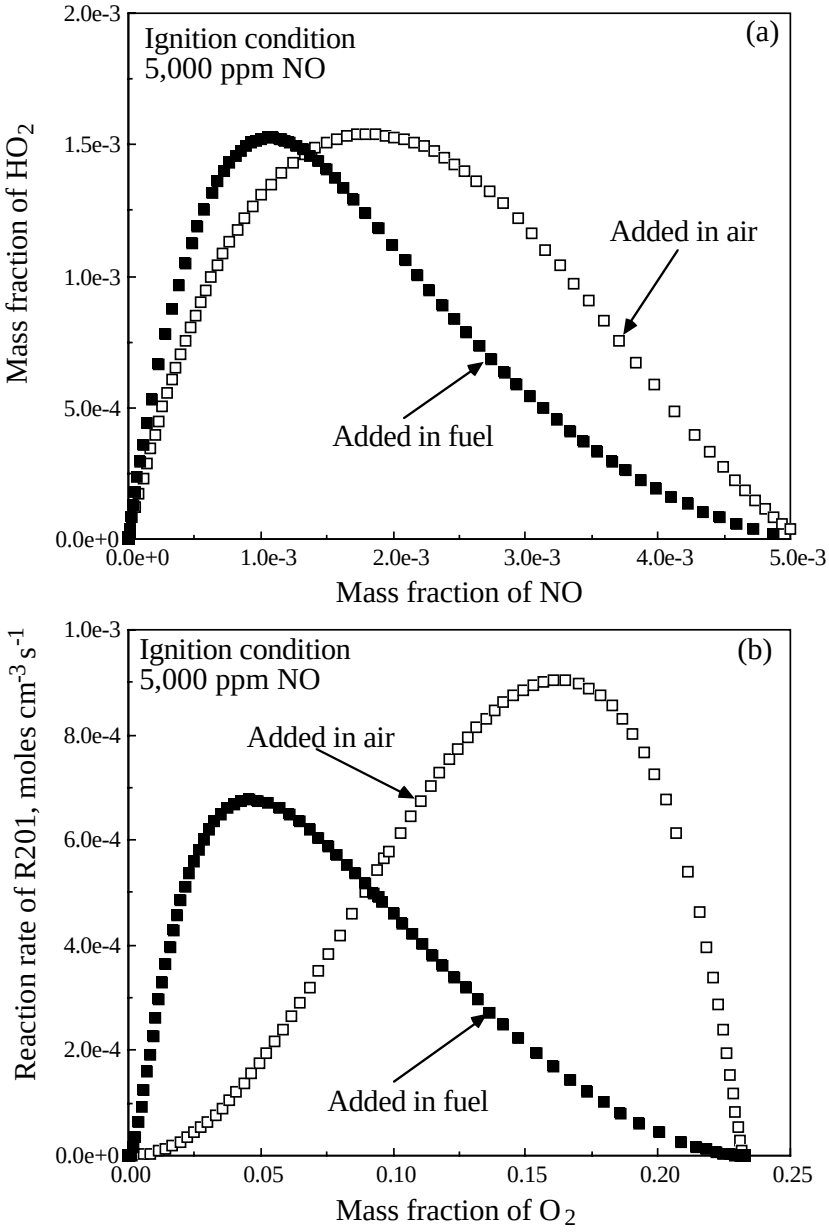

FIG. 7 Variation of (a) mass fraction of HO_2 with mass fraction of NO, and (b) R201 reaction rate with O_2 mass fraction, at the ignition condition of C_2H_4/air, with 5,000 ppm NO addition ($T_{\text{air}} = 1050\,\text{K}$, $T_{\text{fuel}} = 950\,\text{K}$).

of NO addition on the air side. Figure 7b depicts the variation of the reaction rate of R201 with Y_{O_2}, the O_2 mass fraction. The maximum rate of R201 is lower and occurs at lower values of Y_{O_2}, when NO is added on the fuel side, resulting, thus, in lower OH-radical production.

With increasing NO amounts on the fuel side, fuel dilution reduces the HO_2 concentration, reducing the OH production rate through R201. However, this dilution effect is not as strong as in the case of NO addition on the air side. This is as expected, as the same ppm of added NO on the fuel side result in a lower fuel dilution, as compared to the corresponding dilution of O_2 on the air side that already contains large amounts of N_2. As a result, both $\sigma_{\rm ign}$ and $\sigma_{\rm ext}$ are minimally affected when NO is added on the fuel side at amounts ranging from 10,000 to 50,000 ppm.

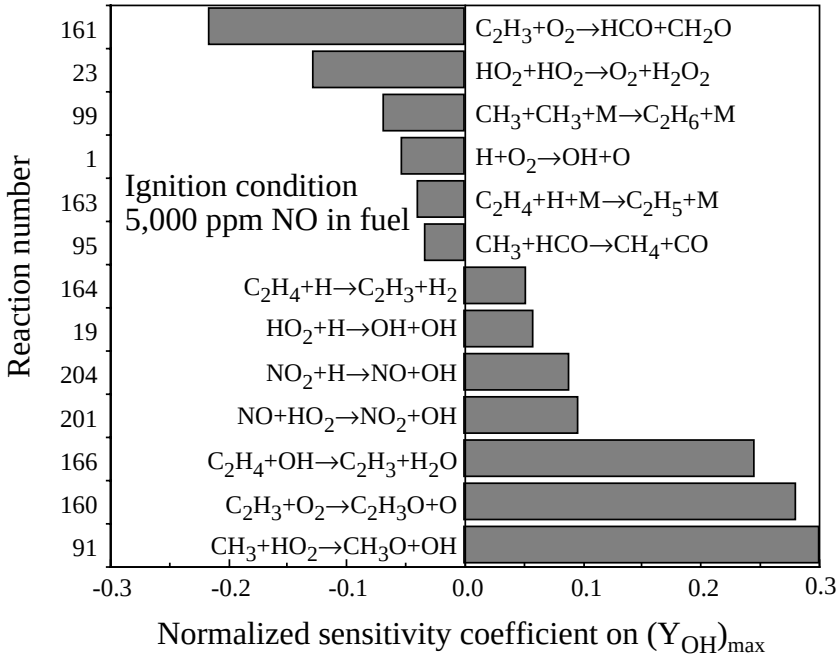

FIG. 8 Normalized sensitivity coefficients on $(Y_{\rm OH})_{\rm max}$ at the ignition condition of C_2H_4/air, with 5,000 ppm NO addition to fuel stream ($T_{\rm air} = 1050\,{\rm K}$, $T_{\rm fuel} = 950\,{\rm K}$).

Figure 8 depicts the normalized sensitivity coefficients of the most important reactions on $(Y_{\rm OH})_{\rm max}$, at the ignition condition for 5,000 ppm NO added to the fuel stream. The effect of R160, R201, R91, R166, R19, and R204 in promoting OH production remains large, but the overall sensitivities are lower compared to the ones shown in Fig. 6. Reactions R161 and R23 also have a retarding effect. We note, however, that while R1 promotes OH production at the conditions of Fig. 6, it plays an inhibiting role at the conditions of Fig. 8. This is a result of the greater need of O_2 for the formation of HO_2, when NO is added to the fuel stream and the R201 rate is reduced, as shown in Fig. 7. Thus, O_2 consumption though R1, while

it has some effect on OH production, reduces its reaction rate in R160, R161, and R50 that are essential for HO_2 formation.

3.3 F_2 addition

In ED98, F_2 addition was found to promote ignition of blends anticipated from thermal cracking of jet fuels, as F radicals increase the consumption rate of hydrocarbons. The results of simulations with 1000 ppm of F_2 on the air side are shown in Fig. 9, along with those obtained for C_2H_4, and for 1000 ppm NO addition, also on the air side.

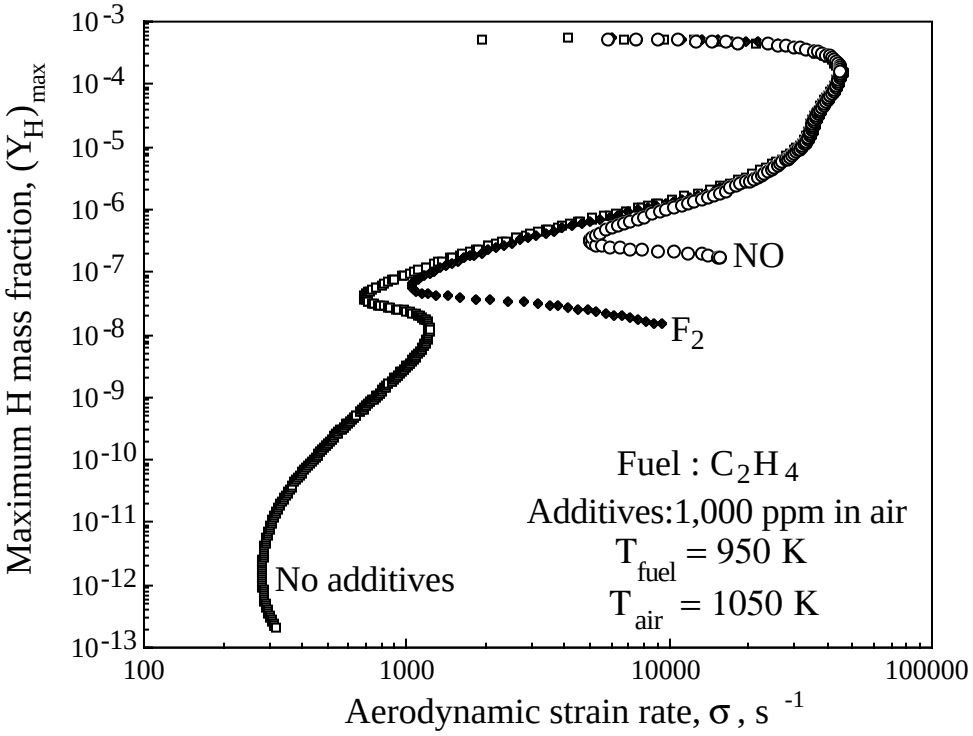

FIG. 9 Effect of 1000 ppm F_2 or NO addition on S-curve response of C_2H_4/air ($T_{\text{air}} = 1050$ K, $T_{\text{fuel}} = 950$ K).

Addition of 1000 ppm of F_2 can be seen to promote C_2H_4 ignition, increasing σ_{ign} by a factor of 3.5. However, it is less effective than addition of 1000 ppm of NO, which increases σ_{ign} by a factor of 16.5. At the ignition point with F_2 addition, fuel is consumed through R166(37%), R165(30%), R163(21%), and

R301 (7%) $\quad C_2H_4 + F \longrightarrow C_2H_3 + HF$.

Ignition is promoted both by the participation of R301 in the fuel consumption, as well as by the additional OH-production mechanism that is active on the air side,

R306 $$H_2O + F \longrightarrow OH + HF\ .$$

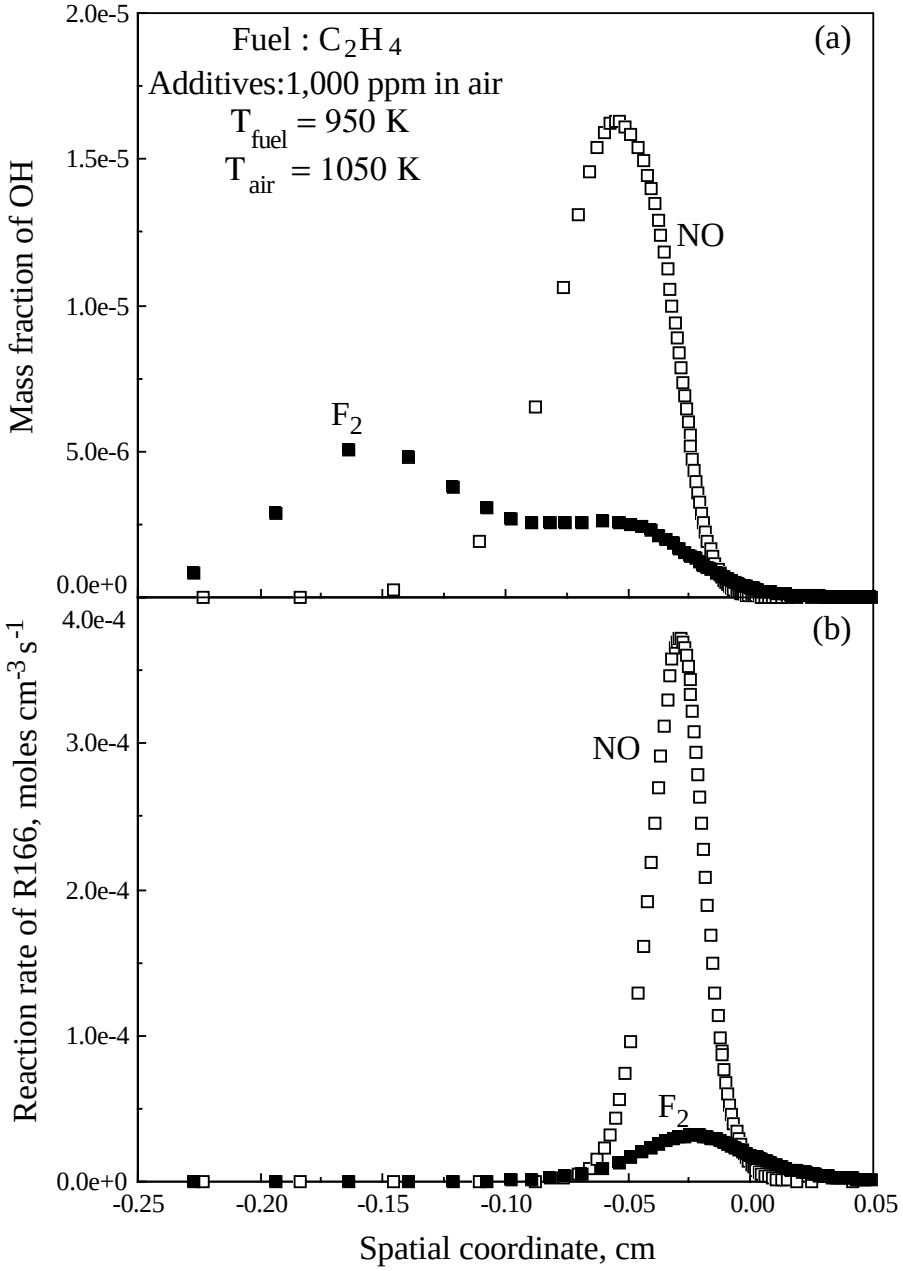

FIG. 10 Spatial variation of (a) mass fraction of OH and (b) rate of reaction R166 at the ignition condition of C_2H_4/air, with independent additions of 1000 ppm of F_2 and NO in air ($T_{\rm air} = 1050\,{\rm K}$, $T_{\rm fuel} = 950\,{\rm K}$).

A comparison of the results of F_2- and NO-addition reveals that the enhanced ignition promotion of NO as compared to F_2 is caused by the higher OH-production rate; a result of R201. OH mass fraction spatial variations at the ignition points, for 1000 ppm additions of F_2 and NO, are shown in Fig. 10a. The higher values for the NO addition can be noted. As a result, the R166 rate is substantially higher for NO addition, as shown in Fig. 10b, thus facilitating the ignition process. It is also interesting to note the peculiar spatial variation of the OH mass fraction for F_2 addition. The initial increase of OH is largely caused by reaction R306 between F radicals and the H_2O produced by R166. The plateau that is subsequently observed is caused by a competition between the consumption of OH through R166 and its production largely through R91.

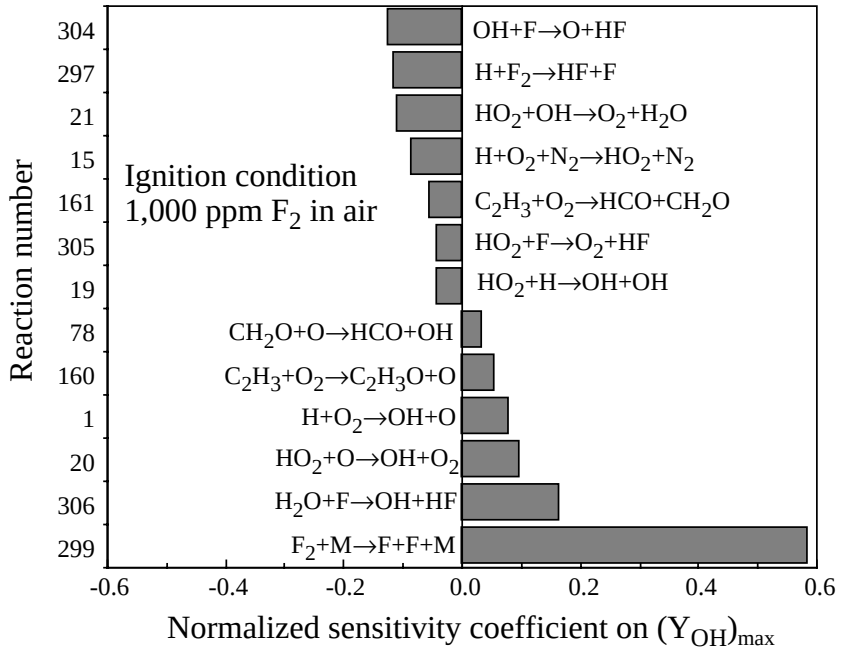

FIG. 11 Normalized sensitivity coefficients on $(Y_{\rm OH})_{\rm max}$ at the ignition condition of C_2H_4/air, with 1000 ppm F_2 addition to the air stream ($T_{\rm air} = 1050\,{\rm K}$, $T_{\rm fuel} = 950\,{\rm K}$).

Figure 11 depicts the normalized sensitivity coefficients of the most important reactions on $(Y_{\rm OH})_{\rm max}$, at the ignition condition with 1000 ppm F_2 added to the air stream. Reactions R1, R306, and

R299 $$F_2 + M \longrightarrow F + F + M \ ,$$

R20 $$HO_2 + O \longrightarrow OH + O_2 ,$$

promote OH production, as R299 is a rate-limiting reaction resulting in F, and R1, R306, and R20 directly produce OH. Reactions R21 and

R304 $$OH + F \longrightarrow O + HF ,$$

R297 $$H + F_2 \longrightarrow HF + F ,$$

R15 $$H + O_2 + N_2 \longrightarrow HO_2 + N_2 ,$$

inhibit OH production. R21 results in stable products, R304 consumes OH radicals as well as F radicals needed by R306, and R297 and R15 consume H radicals needed by R1.

3.4 Simultaneous NO and F_2 addition

The simultaneous presence of NO and F_2 in a reacting flow can result in enhanced radical production through the low activation energy reaction,

R295 $$NO + F_2 \longrightarrow FNO + F .$$

R295 is a hypergolic reaction that can proceed at high rates even at low temperatures (*e.g.*, Mungal & Dimotakis 1984, Dimotakis & Hall 1987). The F radicals produced can facilitate the consumption of the fuel, as described earlier. In ED98, it was found that a simultaneous addition of 10,000 ppm of NO on the fuel-blend side and 10,000 ppm of F_2 on the air side resulted in an increase of $\sigma_{\rm ign}$ by a factor of about 8, to a value of approximately 4000 /s. The fuel blend in those simulations was largely comprised of CH_4 and C_2H_4 in addition to smaller amounts of C_2H_2 and H_2.

Simulations were conducted by adding various amounts of NO on the C_2H_4 side and F_2 on the air side. The results are shown in Fig. 12. The ignition promotion of C_2H_4 is apparent. An equal addition of 10,000 ppm of NO and F_2, for example, results in $\sigma_{\rm ign} = 42{,}000$ /s, an increase by a factor of 140 over the $\sigma_{\rm ign}$ of pure C_2H_4. Recall, that in the absence of F_2, 10,000 ppm of NO added on the fuel

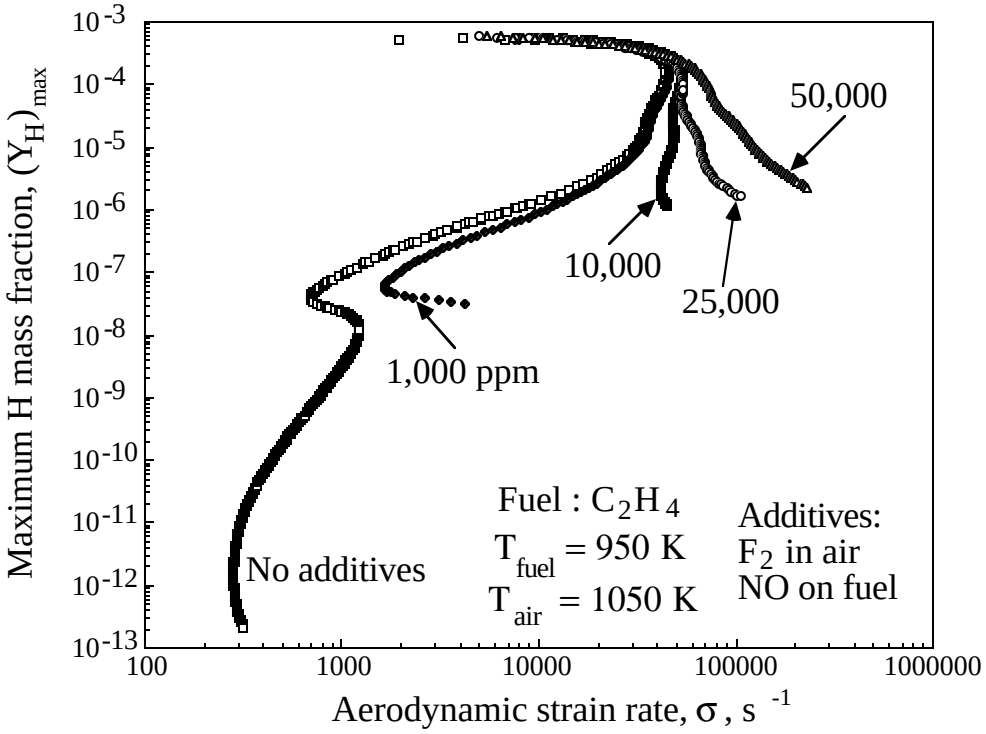

FIG. 12 Effect of simultaneous addition of F_2 to air and NO to fuel streams on S-curve response of C_2H_4/air ($T_{\rm air} = 1050\,{\rm K}$, $T_{\rm fuel} = 950\,{\rm K}$).

side results in $\sigma_{\rm ign} = 27{,}000\,/{\rm s}$, indicating the synergistic effect of F_2 and NO on ignition. The results in Fig. 12 indicate that for additions above 25,000 ppm, the $(C_2H_4 + NO)/(air + F_2)$ system becomes hypergolic, with distinct ignition and extinction conditions that can be identified. Instead, there is a monotonic reduction of the radical concentration as strain rate increases.

Ignition analysis with 10,000 ppm addition reveals that C_2H_4 is consumed through R166(40%), R165(28%), R163(16%), and R301(9%), with NO consumed through R201(85%) and R295(11%), and F_2 consumption through R295(14%) and

R297 (81%) $\qquad\qquad H + F_2 \longrightarrow HF + F$.

The simultaneous presence of NO and F_2 promotes C_2H_4 ignition more effectively than NO alone, with F radicals facilitating C_2H_4 consumption through R301. Subsequent reactions of C_2H_3 produce OH, as described above. OH is, of course, very important in enhancing the main fuel-consuming R166.

The combined effect of F_2 and NO on the fuel consumption process is more profound for larger additions. For example, analysis of a highly-strained condition with 25,000 ppm addition revealed that 21% of the fuel is consumed by R301, compared to 9% for 10,000 ppm addition. Furthermore, the contribution of R295 in NO consumption increases to 32%, from 11% for 10,000 ppm addition. Similarly, 43% of F_2 is consumed by R295. Under such conditions, the overall system became hypergolic, as a result of the hypergolic nature of R295.

The results in Fig. 12 also demonstrate that simultaneous additions of F_2 and NO increase σ_{ext}. This additional resistance to extinction is a result of the enhanced OH production through R306. At the extinction condition, F radicals are produced by R295 and R297.

3.5 H_2 addition

The effect of H_2 addition on C_2H_4 ignition was also studied. The simulations include the addition of 1000 ppm on the fuel side only, to preserve the non-premixed nature of the system. The results are shown in Fig. 13, along with those for pure C_2H_4, and 1000 ppm NO addition to the fuel stream. Although H_2 is an excellent ignition promoter, it is interesting to note the relatively minor increase in σ_{ign}, compared to an addition of a similar amount of NO. The small ignition promotion is caused by the additional H radicals produced as a result of H_2 consumption. By comparison, 1000 ppm of NO on the fuel stream results in an increase of σ_{ign} by a factor of about 4.

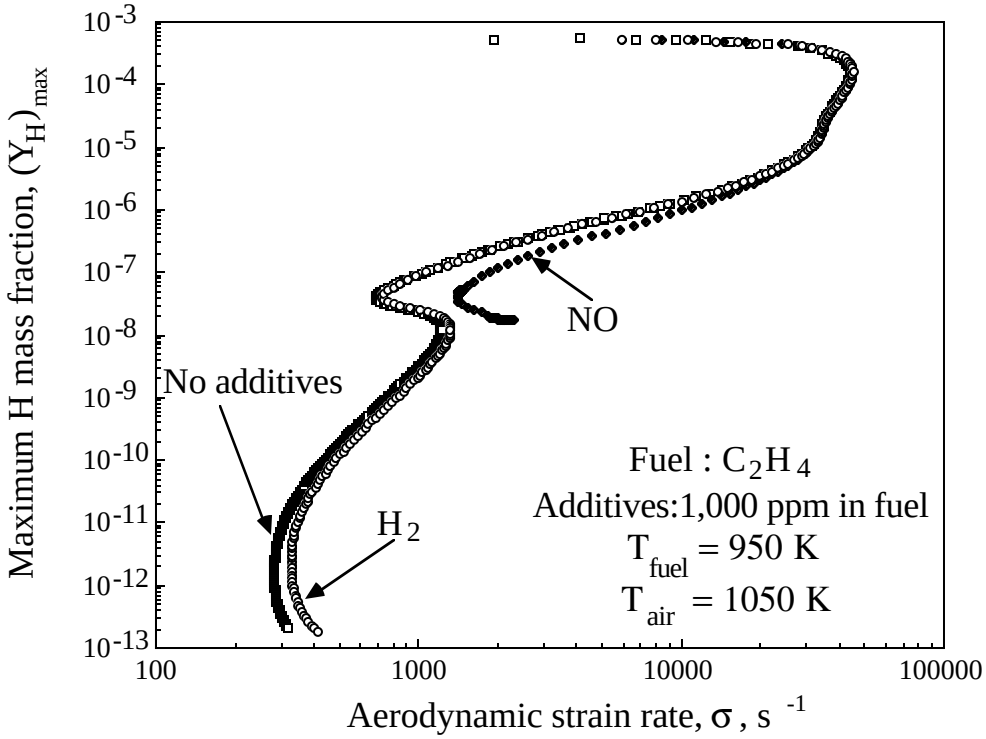

FIG. 13 Influence of 1000 ppm addition of H_2 to fuel stream on S-curve response of C_2H_4/air ($T_{\rm air} = 1050\,{\rm K}$, $T_{\rm fuel} = 950\,{\rm K}$). Comparison with pure C_2H_4 fuel stream and 1000 ppm NO addition to fuel stream.

4. Concluding remarks

The effects of NO, F_2, and H_2 as additives on non-premixed ignition of heated C_2H_4 counterflowing against heated air were numerically investigated for conditions relevant to SCRAMJET's. The simulations were conducted along the stagnation streamline of an opposed-jet configuration with detailed descriptions of molecular transport and chemical kinetics. A two-point continuation approach was implemented, permitting the entire S-curve response to strain rate to be simulated. Simulations were conducted at atmospheric pressure, for free-stream reactant temperatures of $T_{\rm air} = 1050\,{\rm K}$ and $T_{\rm fuel} = 950\,{\rm K}$.

The study reveals that the addition of NO can result in a substantial increase in ignition strain rate, $\sigma_{\rm ign}$, by a factor as high as 120. This substantial ignition promotion is caused by a radical-production mechanism resulting from the interaction between NO and HO_2, the latter being effectively produced during C_2H_4

oxidation. Ignition was found to be very sensitive to small amounts of NO addition, reaching a maximum σ_{ign} at about 10,000 ppm (1%). Higher amounts of NO, up to 50,000 ppm, result in lower σ_{ign} when NO is added to the air stream, while a nearly-constant value is reached with NO in the fuel stream. For amounts less than 10,000 ppm, NO addition to the air stream is more effective in promoting ignition.

Ignition of C_2H_4 with addition of small amounts of F_2 and/or H_2 was also investigated. Although ignition is promoted, the increase in σ_{ign} is substantially less compared to that from NO addition. However, the simultaneous addition of F_2 on the air side and NO on the fuel side further promotes ignition, relative to NO alone, and for additions of about 25,000 ppm, the system becomes hypergolic.

This investigation indicates that ignition can be achieved for strain rates of the order of 32,000 /s by using C_2H_4 and NO. C_2H_4 can be either supplemented or derived from the products of endothermic fuel cracking. Similarly, the small amounts of NO can be added to the air stream. Simultaneous addition of amounts F_2 and NO at a level of 25,000 ppm in C_2H_4, can result in ignition under any strain rate. Such additions would only be required for a brief portion of the SCRAMJET flight profile, corresponding the the lower Mach number regime.

In closing, we recall that the present results are based on the Wang & Frenklach (1997) reaction mechanism that satisfactorily accounts for known C_2H_4 flame behavior. However, there is no clear consensus regarding the oxidation steps controlling C_2H_4 ignition at this time. As discussed above, a major role in the ignition process is played by the vinyoxy radical (CH_2CHO) whose kinetics are not well-established (Wang & Frenklach 1997; Marinov *et al.* 1998; H. Wang 1999, personal communication). There are no flame-ignition/-extinction data available at present, especially for SCRAMJET temperatures, to test such mechanisms in this important regime and we recognize the need to validate the kinetics and our results, which we hope point in the direction of some ignition-enhancement possibilities.

5. Acknowledgments

This study was funded by the Air Force Office of Scientific Research, Air-Breathing Propulsion Program, under Grant F49620–98–1–0052, whose support is gratefully acknowledged.

6. References

Bowman, C. T., Frenklach, M., Gardiner, W. & Smith, G. 1995 The GRI 2.1 Mechanism. pvte. communication.

Bromly, J. H., Barnes, F. J., Mandyczewsky, R., Edwards, T. J. & Haynes, B. S. 1992 An Experimental Investigation of the Mutually Sensitized Oxidation of Nitric Oxide and n-Butane. *Twenty-Fourth Symposium (International) on Combustion* The Combustion Institute, Pittsburgh, 899–907.

Burgess, D. R. F., Zachariah, M. R., Jr., Tsang, W. & Westmoreland, P. R. 1997 Thermochemical and Chemical Kinetic Data for Fluorinated Hydrocarbons. NIST Report.

Dimotakis, P. E. & Hall, J. L. 1987 A simple model for finite chemical kinetics analysis of supersonic turbulent shear layer combustion. *AIAA/SAE/ASME/ASEE* 23rd *Joint Propulsion Meeting*, Paper 87–1879.

Doughty, A., Barnes, F. J., Bromly, J. H. & Haynes, B. S. 1996 The Mutually Sensitized Oxidation of Ethylene and NO: An Experimental and Kinetic Modeling Study. *Twenty-Sixth Symposium (International) on Combustion*. The Combustion Institute, Pittsburgh, 589–596.

Edwards, T. 1996 Fuels and Fuel System Area: Air Force Perspective. AFOSR/-NASA Workshop on Supersonic Scramjet Combustion. 13–16 May 1996, Newport News, VA.

Egolfopoulos, F. N. 1994a Dynamics and Structure of Unsteady, Strained, Laminar Premixed Flames. *Twenty-Fifth Symposium (International) on Combustion* The Combustion Institute, Pittsburgh, 1365–1373.

Egolfopoulos, F. N. 1994b Geometric and Radiation Effects on Steady and Unsteady Strained Laminar Flames. *Twenty-Fifth Symposium (International) on Combustion* The Combustion Institute, Pittsburgh, 1375–1381.

Egolfopoulos, F. N. & Campbell, C. S. 1996 Unsteady, counterflowing, strained diffusion flames: frequency response and scaling. *J. Fluid Mech.* **318**, 1–29.

Egolfopoulos, F. N. & Dimotakis, P. E. 1998 Non-premixed hydrocarbon ignition at high strain rates. *Twenty-Seventh Symposium (International) on Combustion.* The Combustion Institute, Pittsburgh, 641–648.

Egolfopoulos, F. N., Dimotakis, P. E. & Bond, C. L. 1996 On Strained Flames with Hypergolic Reactants: The $H_2/NO/F_2$ System in High-Speed, Supersonic and Subsonic Mixing-Layer Combustion. *Twenty-Sixth Symposium (International) on Combustion.* The Combustion Institute, Pittsburgh, 2885–2893.

Egolfopoulos, F. N., Zhang, H. & Zhang, Z. 1997 Wall Effects on the Propagation and Extinction of Strained, Laminar, Premixed Flames. *Comb. and Flame* **109**, 237–252.

Fotache, C. G., Kreutz, T. G. & Law, C. K. 1997a Ignition of Counterflowing Methane versus Heated Air under Reduced and Elevated Pressures. *Comb. and Flame* **108**, 442–470.

Fotache, C. G., Kreutz, T. G. & Law, C. K. 1997b Ignition of Hydrogen-Enriched Methane versus Heated Air. *Comb. and Flame* **110**, 429–440.

Kee, R. J. 1990 Opposed jet, premixed-flame solver. pvte. communication.

Kee, R. J., Grcar, J. F., Smooke, M. D. & Miller, J. A. 1985 A Fortran program for modeling steady laminar one-dimensional premixed flames. SAND85-8240 DoE report.

Kee, R. J., Rupley, F. M. & Miller J. A. 1989 Chemkin-II: A Fortran Chemical Kinetics Package for the Analysis of Gas-Phase Chemical Kinetics. Sandia Report SAND89–8009.

Kee, R. J., Warnatz, J. & Miller, J. A. 1983 A FORTRAN Computer Code Package for the Evaluation of Gas-Phase Viscosities, Conductivities and Diffusion Coefficients. Sandia Report SAND83–8209.

Kreutz, T. G. & Law, C. K. 1996 Ignition in nonpremixed counterflowing hydrogen versus heated air: Computational study with detailed chemistry. *Comb. and Flame* **104**, 157–175.

Law, C. K. 1998 Chemical Kinetics and Aerodynamics of Ignition. Abstracts, *ARO and AFOSR Contractors' Meeting in Chemical Propulsion* (29 June – 1 July, Long Beach, CA).

Marinov, N., Pitz, W., Westbrook, C., Hori, M. & Matsunaga, N. 1998 An Experimental and Kinetic Calculation of the Promotion Effect of Hydrocarbons on the NO-NO_2 Conversion in a Flow Reactor. *Twenty-Seventh Symposium (International) on Combustion*. The Combustion Institute, Pittsburgh, 389–396.

Mungal, M. G. & Dimotakis, P. E. 1984 Mixing and combustion with low heat release in a turbulent mixing layer. *J. Fluid Mech*. **148**, 349–382.

Nelson, P. F. & Haynes, B. S. 1994 Hydrocarbon-NOx Interactions at Low Temperatures – 1. Conversion of NO to NO_2 Promoted by Propane and the Formation of HNCO. *Twenty-Fifth Symposium (International) on Combustion* The Combustion Institute, Pittsburgh, 1003–1010.

Nishioka, M., Law, C. K. & Takeno, T. 1996 A Flame-Controlling Continuation Method for Generating S-Curve Responses with Detailed Chemistry. *Comb. and Flame* **104**, 328–342.

Tan, Y., Fotache, C. G. & Law, C. K. 1999 Effects of NO on the Ignition of Hydrogen and Hydrocarbons by Heated Counterflowing Air. *Comb. and Flame* (in press).

Wang, H. & Frenklach, M. 1997 A Detailed Kinetic Modeling Study of Aromatics Formation in Laminar Premixed Acetylene and Ethylene Flames. *Comb. and Flame* **110**, 173–221.

Westmoreland, P. R. 1997 pvte. communication.

Williams, F. A. 1985 *Combustion Theory. The Fundamental Theory of Chemically Reacting Flow Systems*. 2^{nd} edition, Benjamin/Cummings, Menlo Park, CA.